

Effects of a Novel Archaeal Tetraether-Based Colipid on the *In Vivo* Gene Transfer Activity of Two Cationic Amphiphiles

Tony Le Gall,^{*,†,‡} Julie Barbeau,[§] Sylvain Barrier,[§] Mathieu Berchel,^{||} Loïc Lemiègre,^{‡,§} Jelena Jeftić,^{‡,§} Cristelle Meriadec,[⊥] Franck Artzner,[⊥] Deborah R. Gill,[#] Stephen C. Hyde,[#] Claude Férec,[†] Pierre Lehn,[†] Paul-Alain Jaffrès,^{‡,||} Thierry Benvegno,^{*,‡,§} and Tristan Montier^{*,†,‡}

[†]Unité INSERM 1078, SFR ScInBioS; Université de Bretagne Occidentale, Université Européenne de Bretagne, 46 rue Félix Le Dantec, CS51819, 29218 Brest Cedex 02, France

[‡]Plateforme SynNanoVect, SFR ScInBioS; Université de Bretagne Occidentale, Université Européenne de Bretagne, Brest, France

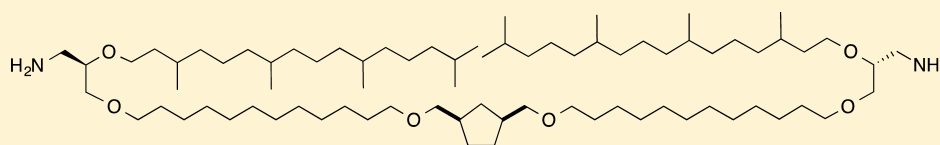
[§]Ecole Nationale Supérieure de Chimie de Rennes, Université Européenne de Bretagne, CNRS, UMR 6226, 11 allée de Beaulieu, CS 50837, 35708 Rennes Cedex 7, France

^{||}CEMCA, CNRS UMR 6521, SFR ScInBioS, Université Européenne de Bretagne, Université de Brest, Brest, France

[⊥]Institut de Physique de Rennes, Université Européenne de Bretagne, Université de Rennes 1, UMR-CNRS 6251, Campus Beaulieu Bat. 11A, 35042 Rennes Cedex, France

[#]Gene Medicine Group, Nuffield Division of Clinical Laboratory Sciences, University of Oxford, John Radcliffe Hospital, Oxford, United Kingdom

Supporting Information



ABSTRACT: Gene therapy for treating inherited diseases like cystic fibrosis might be achieved using multimodular nonviral lipid-based systems. To date, most optimizations have concerned cationic lipids rather than colipids. In this study, an original archaeal tetraether derivative was used as a colipid in combination with one or the other of two monocationic amphiphiles. The liposomes obtained, termed archaeosomes, were characterized regarding lipid self-assembling properties, macroscopic/microscopic structures, DNA condensation/neutralization/relaxation abilities, and colloidal stability in the presence of serum. In addition, gene transfer experiments were conducted in mice with lipid/DNA complexes being administered via systemic or local delivery routes. Altogether, the results showed that the tetraether colipid can provide complexes with different *in vivo* transfection abilities depending on the lipid combination, the lipid/colipid molar ratio, and the administration route. This original colipid appears thus as an innovative modular platform endowed with properties possibly beneficial for fine-tuning of *in vivo* lipofection and other biomedical applications.

KEYWORDS: archaeosome, colipid, cystic fibrosis, DNA, gene delivery, tetraether

1. INTRODUCTION

Gene therapy is a promising strategy to cure a broad range of acquired and inherited diseases, through the delivery into target cells of nucleic acids used as pharmaceutical agents. Besides physical methods,¹ current approaches include the use of viral or synthetic, notably bioinspired, gene delivery systems (for a recent review see ref 2). Among nonviral vectors, cationic liposomes have been widely investigated for *in vitro*^{3–6} as well as *in vivo* transfection assays.^{7–9} Some have been used in clinical trials focusing on diseases such as cystic fibrosis.^{10–12} However, cationic lipid-based formulations, although relatively safe, weakly immunogenic, and well-adapted for large nucleic acid payloads, still suffer from insufficient *in vivo* performance.¹³ Thus, polyfunctional gene delivery systems continue to be developed,^{14,15} notably through the combination of cationic lipids with colipids used as helper compounds.

Cholesterol is usually employed to stabilize liposomal membranes¹⁶ while dioleoyl phosphatidylcholine (DOPC) or dioleoyl phosphatidylethanolamine (DOPE) can be used for enhancing fusogenic properties of lipid assemblies.^{17–19} Indeed, after cellular uptake, a destabilizing effect toward lipid bilayers favors endosomal disruption leading to a better release of DNA into the cytoplasm.²⁰ Structural variations of these helper lipids have been proposed; partially fluorinated DOPE²¹ and terminal benzyl group-bearing DOPC²² analogues showed improved *in vitro* gene transfection activities. DOTMA/Chol-based lipoplexes containing the transdermal penetration enhancer N-

Received: October 25, 2013

Revised: April 11, 2014

Accepted: July 16, 2014

Published: July 16, 2014

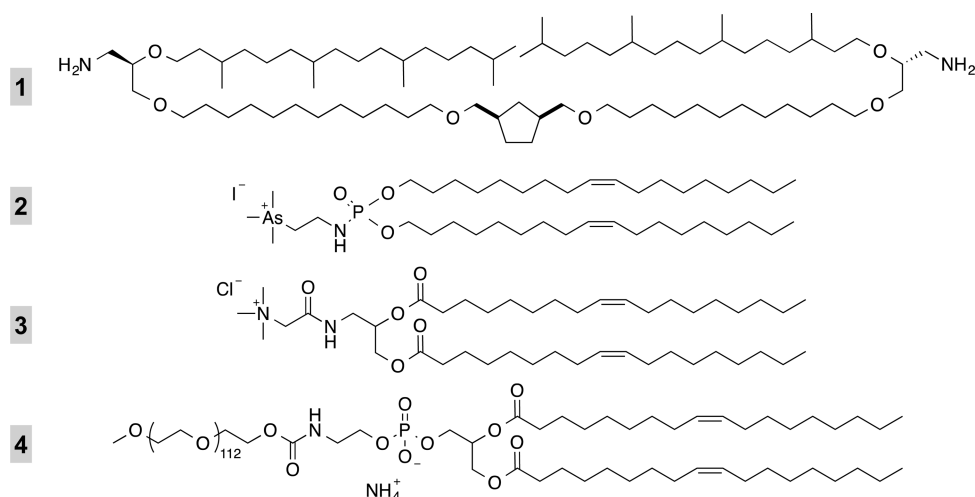


Figure 1. Chemical structures of **1** (archaeal bipolar helper lipid Tetraether,³¹) **2** (arsonium-containing lipophosphoramidate KLN47,³⁰) **3** (glycine betaine-derived cationic lipid MM18, this study), and **4** (commercially available polyethylene glycol (PEG) lipid PE-PEG₅₀₀₀, Avanti Polar Lipids).

lauroylsarcosine instead of DOPE promoted superior *in vitro* and *in vivo* transfection efficiencies together with reduced cell toxicity and hematotoxicity.²³ Incorporation of small amounts of membrane-interacting alkyl phospholipids as helper lipids into cationic liposomes was found to enhance *in vitro* and *in vivo* gene transfer in the context of antitumor therapy.²⁴ Lipophosphoramides incorporating an imidazole polar head were developed as pH-sensitive helper lipids; protonation of this headgroup inside endosomes, leading to a destabilizing effect, may explain the high transfection efficiencies measured.²⁵ More recently, asymmetrical alkyl acyl phosphatidylcholines have been synthesized; complexes incorporating such helper lipids mediated efficient *in vitro* gene transfer.²⁶

Over the past decade, we have developed novel archaeal tetraether lipids as synthetic components of cationic liposomes termed archaeosomes. These artificial bipolar lipids are characterized by (i) an acyclic lipid core composed of two phytanyl chains and a 31 atom long bridging chain containing a cyclopentane ring (supposed to increase the lipid dispersion in water²⁷) linked together by two glycerol moieties to which they are attached via ether bonds and (ii) two polar headgroups at each end of the backbone. A tetraether is a monolayer-forming lipid, i.e., it spans the liposomal membrane from headgroups on one side to headgroups on the other side.²⁸ In contrast to a standard bilayer organization, a single-layer membrane formed by such atypical lipids has a high degree of physical rigidity and chemical/enzymatic stability. We initially reported that archaeal lipids can be used as helpers in combination with conventional, monopolar, cationic lipids to modulate the membrane properties of cationic lipid/DNA complexes and to obtain efficient *in vitro* transfection of eukaryotic cells.^{28,29} *In vivo*, it was thought that tetraether lipids could also enhance the gene transfer activity by (i) providing complexes with some additional rigidity beneficial during extracellular trafficking and (ii) facilitating cellular uptake via endocytosis rather than direct membrane fusion.

In the present work, we investigated the potential of an archaeal bipolar lipid, noted hereafter Tetraether (Figure 1), as a new helper lipid for *in vivo* gene transfer. This monolayer-forming lipid was combined with a monocationic amphiphile, either the previously reported arsonium-containing lipophosphoramidate KLN47³⁰ or the glycine betaine derivative MM18

(whose synthesis is described hereafter). Our objective was to evaluate the impact of Tetraether on the *in vivo* transfection activity of these two different cationic lipids. Thus, we performed a series of physicochemical experiments and *in vivo* transfection studies using either systemic or local delivery routes in mice. Altogether the results obtained revealed the various effects of Tetraether depending on (i) its proportion in mixture with a given cationic lipid, (ii) the cationic lipid with which it is combined, and (iii) the delivery route used.

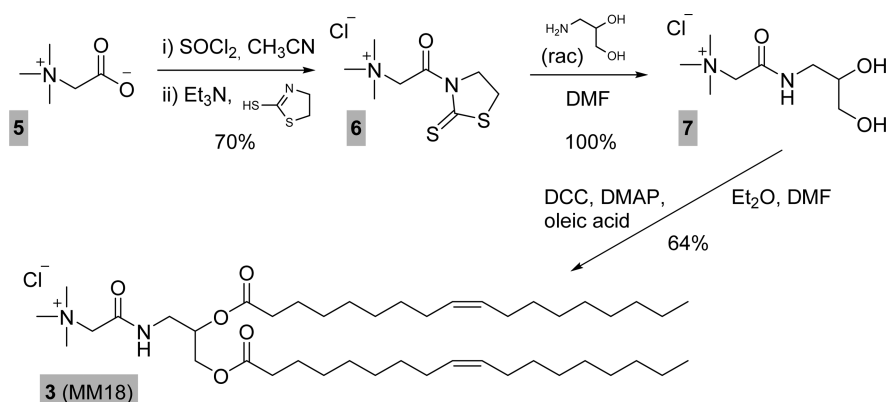
2. EXPERIMENTAL SECTION

2.1. Chemicals. Tetraether³¹ and KLN47³⁰ were prepared as previously described. PE-PEG₅₀₀₀ was purchased from Avanti Polar Lipids. All commercially available chemicals were guaranteed of molecular grade quality; they were used without further purification, and solvents were carefully dried and distilled prior to use.

2.2. DNA. Three different DNAs were used: salmon sperm DNA ($\leq 2,000$ bp; Stratagen), pGL3-Ctrl (5.6 kb; Promega), and pGM144 (9.6 kb;³²). For physicochemical studies, the pGL3-Ctrl and the salmon sperm DNA were used. For *in vivo* transfection experiments, we used the pGM144 (also termed pG4-hCEFI-soLux), which contains synthetic CpG-free sequences comprising a human CMV enhancer coupled to a human elongation factor 1 alpha promoter upstream of a short intron, a codon optimized luciferase cDNA, and a poly(A) BGH sequence.³² All plasmids were amplified in *Escherichia coli* and purified using Qiagen Giga Prep Plasmid Purification protocol (Qiagen, Germany). Plasmid purities were checked by electrophoresis on 0.8% agarose gel. DNA concentrations were estimated spectroscopically by measuring the absorption at 260 nm and confirmed by gel electrophoresis. Preparations showing a value of $OD_{260}/OD_{280} > 1.8$ were used.

2.3. Animals. Six to 9 week old female Swiss mice (Janvier breeding center) were housed and maintained at the University animal facility; they were processed in accordance with the Laboratory Animal Care Guidelines (NIH publication #85-23 revised 1985) and with the agreement of the regional veterinary services (authorization FR; 29-024).

2.4. Chemical Synthesis Process. The cationic glycine betaine derivative MM18 was readily obtained following a three-step process which is depicted in Scheme 1. Unless

Scheme 1. Synthetic Pathway for Obtaining Compound 3 (MM18)^a

^a5, glycine betaine; 6, N-acyl thiazolidine-2-thione; 7, cationic diol.

otherwise stated, nonaqueous reactions were carried out under a nitrogen atmosphere. ¹H and ¹³C NMR spectra were recorded at 400 and 100 MHz, respectively, on a Bruker Avance III, and chemical shifts were calibrated against residual solvent signals of CDCl₃ (δ 7.26 for ¹H NMR, 77.16 for ¹³C) and DMSO (δ 2.50 for ¹H NMR and 39.52 for ¹³C) and reported in ppm. MS spectra were recorded on a Waters Micromass Q-TOF equipped with a Z-spray ion source.

2.5. Synthesis of 3-Betainylthiazolidine-2-thione Chloride (6). Thionyl chloride (1.87 mL, 25.6 mmol, 1.5 equiv) in dry acetonitrile (40 mL) was added dropwise to glycine betaine 5 (2.05 g, 17 mmol, 1 equiv) dissolved in dry acetonitrile (10 mL). The reaction mixture was stirred at 40 °C for 1 h. After concentration under reduced pressure, the resulting acyl chloride (2.90 g, 17 mmol, 1 equiv) was diluted with 20 mL of dry methylene chloride. A mixture of triethylamine (2.39 mL, 17 mmol, 1 equiv) and thiazolidine-2-thione (2.24 g, 18.8 mmol, 1.1 equiv) in 60 mL of dry methylene chloride was added at 0 °C. The reaction mixture was stirred for 30 min at RT, and the solvents were removed under reduced pressure. The residue was washed twice with hot methylene chloride and filtered to yield activated betaine 6 (3.04 g, 70% yield) as a yellow solid: ¹H NMR (400 MHz, DMSO-*d*₆) δ 3.30 (s, 9H, H-1), 3.47–3.51 (t, *J* = 7.6 Hz, 2H, H-5), 4.55–4.60 (t, *J* = 7.6 Hz, 2H, H-4), 5.25 (s, 2H, H-2); ¹³C NMR (DMSO-*d*₆, 100 MHz) δ 28.89 (C-4), 52.96 (C-1), 55.43 (C-5), 66.54 (C-2), 165.01 (C-3), 202.11 (C-6); LSIMS calcd for [C₈H₁₃ON₂S₂Cl]⁺ 219.0626, found 219.0623.

2.6. Synthesis of 1-Betainylaminopropane-2,3-diol Chloride (7). Aminopropanediol (578 mg, 6.35 mmol, 1 equiv) was dissolved in dry DMF (60 mL) and cooled to 0 °C. Activated betaine 6 (1.78 g, 6.98 mmol, 1.1 equiv) was added gradually, and the reaction mixture was stirred at 0 °C for 2 h. DMF was removed under reduced pressure, and the residue was taken with a mixture of H₂O/NH₃ (32%) (25/1: v/v), stirred for 30 min, then washed with ethyl acetate, and lyophilized to yield compound 7 (1.8 g, quantitative yield) as a brown oil: ¹H NMR (400 MHz, DMSO-*d*₆) δ 2.98–3.04 (m, 1H, H-4 α), 3.22 (s, 9H, H-1), 3.26–3.36 (m, 3H, H-4 β , H-6), 3.51–3.53 (m, 1H, H-5), 4.16 (s, 2H, H-2), 8.87 (sl, 1H, NH); ¹³C NMR (DMSO-*d*₆, 100 MHz) δ 42.33 (C-4), 53.31 (C-1), 63.66 (C-6), 64.16 (C-2), 69.96 (C-5), 163.37 (C-3).

2.7. Synthesis of 1-Betainylamino-2,3-dioleoyloxypropane Chloride (3). Oleic acid (2.22 g, 7.8 mmol, 3 equiv) was added to DCC (2.15 g, 10 mmol, 4 equiv) and DMAP (223

mg, 1.83 mmol, 0.7 equiv) dispersed in dry diethyl ether (20 mL). The reaction mixture was stirred at RT for 1 h, and compound 7 (593 mg, 2.6 mmol, 1 equiv) dissolved in dry DMF (25 mL) was added dropwise. After 3 days at RT, the organic solvent was removed under reduced pressure. The residue was dissolved in a mixture of hexane/butanol (1/1: v/v), and the organic layers were washed with a saturated aqueous solution of brine, dried (MgSO₄), and concentrated under reduced pressure. Flash column chromatography on silica gel (CH₂Cl₂/MeOH: 9/1) yielded compound 3 (MM18) as a white powder (1.25 g, 64% yield): ¹H NMR (400 MHz, CDCl₃) δ 0.83–0.87 (m, 6H, H-14, H-22), 1.22–1.26 (2s, 40H, (CH₂)₄, (CH₂)₆), 1.57 (m, 4H, H-9, H-17), 1.98 (m, 8H, H-10, H-13, H-18, H-21), 2.26–2.38 (m, 4H, H-8, H-16), 3.35 (m, 1H, H-4 α), 3.43 (s, 9H, H-1), 3.60–3.64 (m, 1H, H-4 β), 4.04–4.10 (m, 2H, H-6), 4.23–4.26 (m, 2H, H-2), 5.13–5.18 (m, 1H, H-5), 5.28–5.36 (m, 4H, H-11, H-12, H-19, H-20), 9.20 (sl, 1H, NH); ¹³C NMR (CDCl₃, 100 MHz) δ 14.05 (C-14, C-22), 27.15–31.83 (20 CH₂, C-9, C-10, C-13, C-17, C-18, C-21), 34.18 (C-8, C-16), 40.21 (C-4), 54.61 (C-1), 62.82 (C-6), 64.71 (C-2), 70.70 (C-5), 129.93 (C-11, C-12, C-19, C-20), 163.76 (C-3), 173.40 (C-7, C-15); ESIMS calcd for [C₄₄H₈₃N₂O₅]⁺ 719.6302, found 717.6296.

2.8. Preparation of Cationic Liposomes and Lipid/DNA Complexes. Lipid mixtures were prepared at a 20 mM final concentration by dissolving the required amount of lipid in chloroform. The organic solvents were removed under reduced pressure to form a lipid film, which was further dried under vacuum overnight to remove traces of the solvents. Liposomes were formed by hydrating lipid films with freshly distilled water at RT and were stored at 4 °C for 24 h. Formulations were sonicated at 40 °C for 10 min using an ultrasonic bath (FB15051) at 80 Hz. Complexes were prepared at RT by adding, in water or in 0.9% NaCl, DNA (salmon sperm, nonsonicated, DNA or pDNA) onto liposomes.

2.9. X-ray Diffraction. X-ray scattering experiments (pure aqueous MM18, KLN47 and Tetraether-based solutions) were performed using a FR591 Bruker AXS X-ray generator with a monochromatic Cu K α radiation (λ = 1.541 Å) and point collimation. X-ray patterns were collected with a Mar345 Image-Plate detector (Marresearch, Norderstedt, Germany). The X-ray patterns were therefore recorded for a range of reciprocal spacing $q = 4\pi \sin \theta/\lambda$ from 0.03 to 1.6 Å⁻¹ where θ is the diffraction angle. The repeat distances $d = 2\pi/q$ should be between 200 and 3.9 Å. The samples were placed into 1 mm

glass capillaries (Glas W. Müller, Germany). The X-ray beam was positioned at several points of the capillary to assess the homogeneity of the preparation. MM18 or KLN47/Tetraether mixture (10/1; mol/mol) studies were performed on the small-angle scattering instrument SWING at SOLEIL (Synchrotron SOLEIL, Saint-Aubin, Gif-sur-Yvette, France). Swing line characteristics were as follows: energy = 12 keV, wavelength = 1.0332 Å, distance between the sample and the detector = 1.2 m, and acquisition time = 100 ms. Concentration of the solutions analyzed was 100 mg/mL.

2.10. Electrophoretic and Dynamic Light Scattering (DLS). The average volume diameter, polydispersity index (defined as the variance of the log-normal distribution of particle sizes), zeta-potential, and electrophoretic mobility of liposomes and lipid/DNA complexes were measured by dynamic light scattering (DLS) using a Delsa Nano (Beckman Coulter apparatus) or a 3,000 Zetasizer (Malvern Instruments) at 25 °C. The samples were analyzed pure (without any dilution) or after an appropriate dilution of the formulations.

2.11. DNA Condensation and Relaxation. The condensation of a pDNA by the formulations studied was investigated using ethidium bromide intercalation into DNA. Upon condensation, ethidium bromide is expelled from DNA and thus the fluorescence signal decreases. Conversely, DNA relaxation from the complexes results in recovery of fluorescence.³³ These assays were performed in 96-well plates in water. The maximum fluorescence signal was obtained when ethidium bromide (1.5 µg/mL final) was bound to free pDNA (1.0 µg/well). DNA was added to the wells containing different amounts of the reagents in order to form complexes characterized by different charge ratios. As a negative control, some wells were added with free ethidium bromide at the same concentration. The fluorescence signals were measured using a Fluoroskan Ascent FL plate reader (ThermoElectron Instruments, France) at an excitation wavelength of 530 nm and an emission wavelength of 590 nm. The resistance of the complexes formed to dissociation was studied by using dextran sulfate (MW > 500,000, Sigma-Aldrich) as a counteranion competing with pDNA for electrostatic interaction with the cationic lipids. Last, DNA retardations were assessed by agarose gel electrophoresis shift assay.

2.12. Aggregation of Lipid/DNA Complexes in the Presence of Serum. Transparent to turbid medium changes were used as an indicator of aggregation/precipitation. Complexes were formed in 0.9% NaCl, as described above, before addition of native fetal bovine serum (FBS). As controls, some DNA containing wells were also added with serum and other wells containing the same complexes were added with 0.9% NaCl. Optical densities were determined at 630 nm and at 25 °C using a Multiskan Spectrum plate reader (Thermo-Electron Instrument). Measurements were done at regular time intervals following the addition of serum to the wells.

2.13. Cryo-Transmission Electron Microscopy (Cryo-TEM). Five microliter samples (liposomes or lipid/DNA complexes; lipid concentration: 1 mg/mL) were deposited onto a holey carbon coated copper grid; the excess was blotted with a filter paper, and the grid was plunged into a liquid ethane bath cooled with liquid nitrogen (Leica EM CPC). Specimens were maintained at ~-170 °C using a cryo holder (Gatan). They were observed with an FEI Technai F20 electron microscope operating at 200 kV and at a nominal magnification of 50000× under low dose conditions. Images were recorded with a 2K × 2K Gatan slow scan CCD camera.

2.14. In Vivo Transfections. For iv injections, complexes were prepared at RT, in 0.9% NaCl, at CR4. Animals were placed in a restrainer, and then 300 µL of complexes incorporating 50 µg of pDNA was iv injected per mouse, via the tail vein, within 5 to 10 s, using a 1/2 in. 26-gauge needle and a 1 mL syringe. For i.n. depositions, complexes were prepared at RT, in water, at CR3. Here, PE-PEG₅₀₀₀ was required to obtain highly concentrated, sterically stabilized, complexes. Animals were first anesthetized with ketamine/xylazine (40 mg/kg animal; intraperitoneal (ip)), and then 25 µL of complexes incorporating 25 µg of DNA was instilled per mouse, via the right nostril within 15–30 min, using a catheter (<0.5 mm outer diameter) connected to a 100 µL syringe (Hamilton 1710RN) mounted on a pump (Harvard Apparatus). Once administered, animals were placed in a box near a heat source until they recovered from anesthesia. A total of three to six mice were treated with each formulation; four mice received naked uncomplexed DNA delivered via iv or i.n. route.

2.15. In Vivo Bioluminescence: Noninvasive Imaging of Luciferase Activity. Mice received first an ip injection of luciferin (0.16 g/kg animal; Interchim). Three minutes later, animals were anesthetized by isoflurane inhalation (4% air–isoflurane blend) or ketamine/xylazine injection (40 mg/kg animal; ip). Next, animals were laid inside the acquisition chamber of an *in vivo* imaging system equipped with a cooled, slow-scan, CCD camera (NightOwl, Berthold) and driven with associated software (WinLight 32, Berthold). Five minutes after luciferin injection, luminescence images were captured at 8 × 8 binning with exposure times ranging from 2 to 4 min, depending on the luminescence intensity. Finally, luminescence images were superimposed onto still images of each mouse. Signal intensities were quantified within the regions of interest as relative light units (RLU).

2.16. In Vivo Side Effects. ALT (alanine aminotransferase) and AST (aspartate amino transferase) activities were measured in plasma 24 h and a few days after administration. Briefly, blood samples (~100 µL) were collected from the saphenous vein using Microvettes CB300 (Sarstedt). They were then centrifuged at 10000g for 2 min at 4 °C in order to isolate plasma from cell pellet. The Elitech kit (Elitech) together with the Selectra E apparatus (Elitech) was used to measure, according to the manufacturer's protocol, the NADH to NAD conversion that operates when transaminases are in the presence of their respective substrates. Results were expressed in International Units per liter (IU/L).

3. RESULTS

The formulations prepared in this study were based on MM18 and KLN47 cationic lipids used either pure or in combination with Tetraether (which is under a cationic form at pH 7.0, under physiological conditions). The chemical syntheses of KLN47³⁰ and Tetraether³¹ were previously described, but not that of MM18. Thus, we first describe hereafter the synthesis of MM18. We next report some physicochemical characteristics of the various lipid-based formulations prepared. Finally, these preparations were used to perform several *in vivo* gene transfection experiments in mice.

3.1. Synthesis of 3 (MM18). Cationic lipid 3 is characterized by the naturally occurring glycine betaine polar head linked to two unsaturated oleic fatty chains through an aminopropanediol spacer. Glycine betaine 5 was converted into the reactive electrophilic *N*-acyl thiazolidine-2-thione 6.³⁴

Commercially available 3-amino-1,2-propanediol (racemic) was quantitatively *N*-acylated by reagent **6** to give the cationic diol **7** under mild conditions. The cationic lipid **3** (MM18) was finally obtained in a second step (64% yield) by reacting **7** with **3** equiv of oleic acid using standard DCC/DMAP coupling conditions (Scheme 1).

3.2. Physicochemical Studies. **3.2.1. Formulation and Colloidal Stability of Liposomes and Archaeosomes.** Aqueous solutions of lipids were prepared at high concentration (20 mM of cationic lipid) using the film hydration method, as previously described.⁷ Sonication cycles (each for 10 min at 40 °C) provided homogeneous cationic vesicle solutions. Thus, we prepared various formulations containing exclusively a cationic lipid (MM18 or KLN47) or a combination of one of these two cationic lipids with Tetraether colipid, the cationic lipid/colipid molar ratio being set at 10/1, 10/2, or 10/3. As shown in Table 1, nanoparticles bearing a

Table 1. Size and Zeta-Potential of Liposomes and Archaeosomes Prepared at High Concentration^a

entry	sample (mol/mol)	size ^{b/c} (nm)	poly. index ^{b/c}	Zeta (mV) ^b
1	KLN47	57/58	0.27/0.30	+63
2	KLN47/Tetraether (10/1)	242/203	0.29/0.25	+77
3	MM18	68/65	0.23/0.27	+85
4	MM18/Tetraether (10/1)	190/166	0.27/0.30	+95
5	MM18/Tetraether (10/2)	220/nd	0.25/nd	+105
6	MM18/Tetraether (10/3)	250/nd	0.28/nd	+94

^aLiposomes and archaeosomes formed in water at 20 nmol[+]/μL of cationic lipid (either KLN47 or MM18). nd, not determined (means with $n = 3$; deviations $\leq 10\%$). ^bMeasurements performed immediately after liposomal preparation. ^cMeasurements performed at least 1 month after liposomal preparation.

positive surface charge were observed in every instance. Archaeosomes were slightly more positive and ~ 2.5 to 4.0 times bigger than corresponding liposomes. As concerns MM18 archaeosomes, a slight increase in size was observed with the amount of colipid. On the contrary, despite Tetraether being under a cationic form, the zeta potential did not clearly increase with the increase of Tetraether proportion. Hence, the positive charge of archaeosomes mainly resulted from the cationic lipid (MM18 or KLN47).

All these values remained identical over at least one month (during storage at 4 °C). At the same time, the *in vitro* transfection efficiency of these preparations remained at high level (Figure S1 in the Supporting Information). Altogether, these results indicate that all the formulations studied exhibited long-term colloidal and functional stability.

3.2.2. Small Angle X-ray Scattering (SAXS) and Wide Angle X-ray Scattering (WAXS) Analyses of Liposomes and Archaeosomes. The influence of the helper lipid on the lyotropic self-assembling properties of each cationic lipid was evaluated by X-ray diffraction.

For this purpose, lipid-based aqueous solutions were prepared at high concentration (100 mg/mL). All samples were sonicated and thermal cycles were performed in order to ensure homogeneity. MM18 and KLN47-based liposomes were studied with a FR591 Bruker AXS generator (ENSCR, France) whereas scattering measurements using MM18 or KLN47-based archaeosomes (in a lipid/colipid molar ratio of 10/1) were performed on the small-angle scattering instrument SWING at Synchrotron SOLEIL (France), as described in the Experimental Section. The results obtained are shown in Figure 2. Pure MM18 formed hexagonal inverted phase H_{II} as shown in Figure 2A, for which the pattern of peaks $1q:\sqrt{3}q:\sqrt{4}q:\sqrt{7}q$ is typical. The neat KLN47 spectrum is shown in Figure 2B, the succession of peaks $1q:2q:3q:4q$ being a clear signature of a lamellar fluid phase L_{α} . In the case of

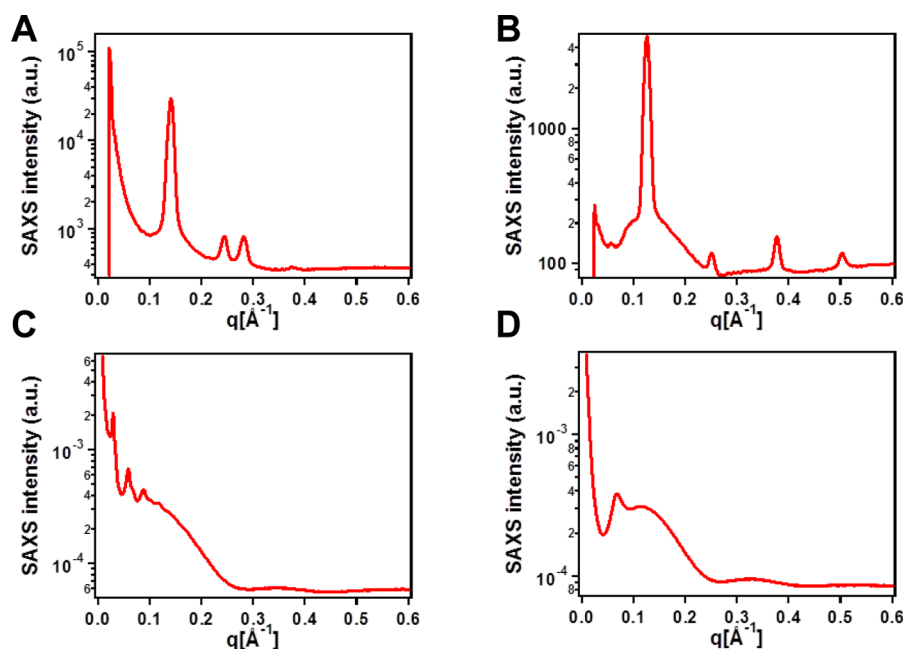


Figure 2. Representative spectra of SAXS and WAXS measurements obtained with MM18 (A), KLN47 (B), MM18/Tetraether 10/1 (C), and KLN47/Tetraether 10/1 (D). Data were obtained at room temperature (RT). (A) Neat spectrum of MM18 showing inverted hexagonal phase H_{II} ; (B) neat lipid KLN47 in the lamellar fluid phase L_{α} ; (C) MM18/Tetraether mixture showing lamellar fluid phase L_{α} coexisting with lamellar swollen phase L_s ; (D) KLN47/Tetraether mixture exhibiting a large extent of lamellar swollen phase L_s .

MM18, upon addition of Tetraether, the phase changed to a lamellar fluid phase L_{α} with some extent of a swollen phase L_s , for which the amount of water is significant. The large peak observed is a signature of the presence of a swollen phase, as deduced from the spectrum shown in Figure 2C. On the contrary, both KLN47 and KLN47/Tetraether exhibited a lamellar phase (Figures 2B and 2D). However, the fluid lamellar phase L_{α} (less hydrated) observed with KLN47 was distinguishable from the swollen lamellar phase L_s (more hydrated) observed with KLN47/Tetraether. To assign the spectrum, the large peak observed in the small angle region $0.0\text{--}0.3 \text{ \AA}^{-1}$ is a signature of a lamellar swollen phase L_s . The swollen phase emerged from the favored hydration thanks to the important charge density of the polar head. This was especially the case for MM18, the charge density of MM18 liposomes (+85 mV) being clearly higher than that of KLN47 liposomes (+63 mV, Table 1). The fact that MM18 was more readily hydrated than KLN47, enough to invert the phase, may be explained by the charge distribution of their respective polar headgroups. Indeed, the N^+/Cl^- ion pair in MM18 is more polar and allows a better hydration than the As^+/I^- ion pair in KLN47. Thus, the interlamellar distance d can be expected for the two lipids to be as follows: $d(\text{MM18}) > d(\text{KLN47})$. This distance was determined from the relation $d = 2\pi/q$ where q is the position of the first peak in the spectrum. It is noteworthy that d is larger in the MM18-based system ($d = 212 \text{ \AA}$; Figure 2C) compared to the KLN47/Tetraether mixture ($d = 92 \text{ \AA}$; Figure 2D). Clearly, combining KLN47 and MM18 with Tetraether impacted on their respective organization (Figure 2A–D). For the swollen phases where the organization is less pronounced because the lamellas are well hydrated and behave more independently, there are fewer stacking interactions, so they may readily enroll into vesicles. In summary, Tetraether has a significant lyotropic effect on the self-assembling properties of KLN47 and MM18, which in turn may impact on the *in vivo* behavior of archaeosomes and archaeoplexes.

3.2.3. Formulation and Colloidal Stability of Lipid/DNA Complexes. Lipoplexes (mixtures of KLN47 or MM18 with DNA) and archaeoplexes (mixtures of KLN47/Tetraether or MM18/Tetraether with DNA) were characterized regarding size and surface charge. The aim was to identify experimental conditions that allowed obtaining complexes suitable for *in vivo* administrations in subsequent experiments. To calculate the mean theoretical charge ratio (CR, +/-), which is the ratio of the positive charges provided by the polar headgroup of the vector to the negative DNA phosphate charges, we assumed that (i) $1 \mu\text{g}$ of DNA is 3 nmol of negatively charged phosphate and (ii) one permanent positive charge is displayed by each cationic lipid (Tetraether positive charges were not taken into account in these calculations). For intravenous (iv) injections, complexes were prepared by mixing, in saline solution, cationic lipids and DNA at CR4. Indeed, we have previously shown that such a charge ratio can allow obtaining efficient transfection of the lungs *in vivo* via this route.^{7,8} As shown in Table 2, although DNA addition led to a decrease of zeta-potential value, each complex exhibited a clearly positive surface charge with a relatively small size; neither aggregation nor precipitation occurred after 10 min at RT.

For intranasal (i.n.) deposition, complexes were to be sterically stabilized since they were prepared in a smaller volume and DNA concentration was higher than for iv injection. For this purpose, PE-PEG₅₀₀₀ (see Figure 1) was added to lipid formulations a few minutes before mixing with

Table 2. Size and Zeta-Potential of Lipid/DNA Complexes As Prepared for Iv Injection^a

entry	sample (mol/mol)	size (nm)	poly. index	zeta (mV)
1	KLN47	180	0.28	+37
2	KLN47/Tetraether (10/1)	340	0.28	+30
3	MM18	240	0.26	+25
4	MM18/Tetraether (10/1)	180	0.17	+39
5	MM18/Tetraether (10/2)	172	0.23	+76
6	MM18/Tetraether (10/3)	210	0.22	nd

^aComplexes formed in 0.9% NaCl at CR4 using salmon sperm DNA; final concentrations of cationic lipid and DNA of 2.0 nmol/ μL and 0.2 $\mu\text{g}/\mu\text{L}$, respectively (means with $n = 3$; deviations $\leq 10\%$).

DNA. Complexes were prepared in water at CR3, because both the smaller volume that can be administered and the higher DNA concentration did not allow testing at CR4. As reported in Table 3, all complexes exhibited clearly positive zeta-

Table 3. Size and Zeta-Potential of PEGylated Lipid/DNA Complexes As Prepared for I.n. Deposition^a

entry	sample (mol/mol)	size (nm)	poly. index	zeta (mV)
1	KLN47	162	0.23	+40
2	KLN47/Tetraether (10/1)	219	0.37	+42
3	MM18	108	0.10	+45
4	MM18/Tetraether (10/1)	230	0.42	+44

^aComplexes formed in water at CR3 using pGL3-Ctrl plasmid DNA (pDNA); final concentrations of cationic lipid, PE-PEG₅₀₀₀ and DNA of 9 nmol/ μL , 2 $\mu\text{g}/\mu\text{L}$, and 1 $\mu\text{g}/\mu\text{L}$, respectively (means with $n = 3$; deviations $\leq 10\%$).

potential values and their sizes were of the same order of magnitude as those prepared according to iv procedure. A size increase effect attributable to Tetraether was observed.

3.2.4. DNA Condensation, Neutralization, and Relaxation Assays. Ethidium bromide exclusion assays were performed to characterize the interaction of the various lipid-based formulations studied with DNA. First, the various lipid-based formulations were used to form lipid/DNA complexes under experimental conditions similar to those used for preparing complexes to be delivered iv in animals, i.e., in 0.9% NaCl and at CR4. The results obtained showed that all formulations were able to perform DNA condensation, although some differences were evidenced (Figure 3).

Figure 3 shows the results obtained using complexes formed at CR4; the results obtained at three other charge ratios are provided in Figure S2 in the Supporting Information. When LFM was used, DNA condensation was rapid and efficient, but it proved to be unstable over time (a progressive fluorescence recovery being noticed ~ 1 h after addition of the DNA to the cationic lipid), as we have previously reported.⁷ Using other formulations, various DNA condensation performances were observed, but in contrast to LFM, they all progressively improved over time (fluorescence values decreasing up to ~ 5 h after mixing). KLN47 (combined or not with Tetraether) demonstrated efficient condensation abilities, reaching the lowest fluorescence measured ($\sim 5\%$ residual fluorescence at 10 h; Figure 3A). When using MM18, a few minutes after mixing with DNA, condensation was poorly efficient, even less when using Tetraether-based formulations (regardless of the lipid/colipid molar ratio). However, these condensations improved over time: since 1–2 h, residual fluorescence

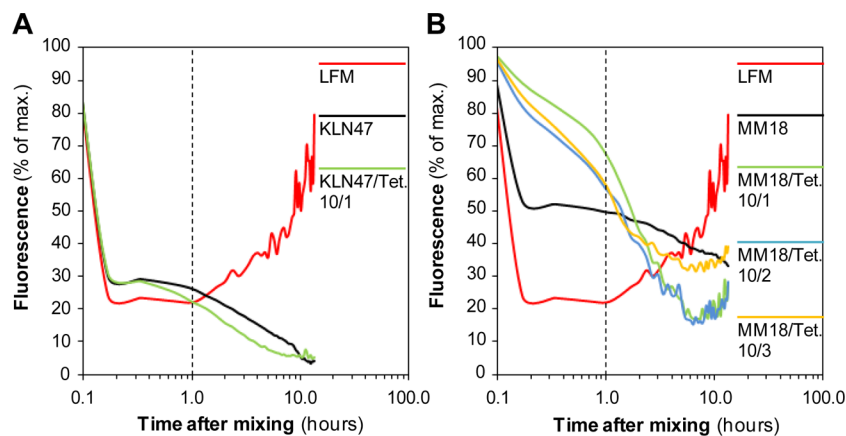


Figure 3. Kinetics of DNA condensation within lipoplexes and archaeoplexes. KLN47 (A) and MM18 (B)-based formulations were mixed in 0.9% NaCl with pGL3-Ctrl at CR4. The fluorescence decrease allowed monitoring DNA entrapment within the complexes formed. DNA condensation was evaluated for 14 h, with measurements repeated every 20 min. Data are expressed as a percentage of the maximum fluorescence, i.e., the fluorescence observed when ethidium bromide is intercalated into DNA in the absence of any cationic lipid. The commercial lipofection reagent Lipofectamine (LFM, Invitrogen) was used as a reference; naked pDNA (100% fluorescence) and water (0%) were used as controls (means with $n = 3$).

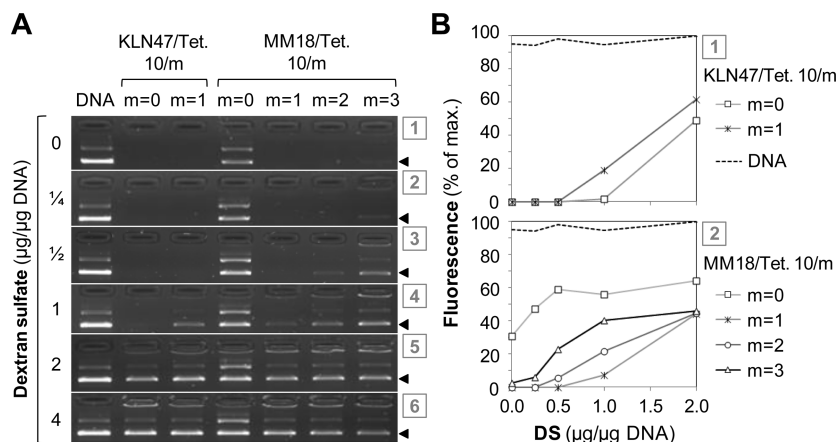


Figure 4. DNA condensation/neutralization and resistance of lipoplexes to dissociation. KLN47 and MM18-based formulations were mixed in 0.9% NaCl with pGL3-Ctrl at CR4. After ~ 1 h at RT, the complexes formed were incubated with increasing quantities of dextran sulfate (DS) before performing agarose gel electrophoresis (A). The fluorescence of the faster (lower) DNA band (arrow; corresponding to a supercoiled pDNA conformation) is expressed as a percentage of the band signal obtained with naked (uncomplexed) DNA (B). m , proportion of Tetraether.

dropped down to $\sim 50\%$ and, thereafter, condensations became even better within archaeoplexes than within lipoplexes (Figure 3B). Such condensation kinetics indicate that some progressive self-organizations can occur between liposomes and DNA, especially when using MM18/Tetraether-based formulations. Finally, this experiment emphasizes that a lag time may be observed in order to obtain, regardless of the formulation, at least 50% of DNA condensation. Consequently, lipid/DNA complexes were systematically left at RT for ~ 1 h before being used in subsequent experiments.

Next, agarose gel electrophoresis shift assays were conducted in order to determine for the various lipid-based formulations studied (i) their DNA condensation/neutralization ability and (ii) the resistance of their complexes with DNA in the presence of an anionic polymer (dextran sulfate) mimicking the extracellular matrix (Figure 4).

The results showed some consistencies with those of our above-mentioned condensation assays (Figure 3). Indeed, when diluted in saline solution, DNA was efficiently neutralized by all formulations except one: neutralization was only partial with MM18 whereas no fluorescence was detectable on the gel when

using all the other formulations (Figure 4A1; see also Figure S3 in the Supporting Information). Thus, Tetraether strongly enhanced the DNA neutralization ability of MM18 whereas it did not impact on that of KLN47. As concerns resistance to dissociation, different effects were observed, depending once again on both the type of cationic lipid and the lipid/colipid proportion. When combined with KLN47, Tetraether provided some instability, archaeoplexes relaxing at a lower dose (from 1 $\mu\text{g}/\mu\text{g}$ DNA) than lipoplexes (from 2 $\mu\text{g}/\mu\text{g}$ DNA; Figure 4B1). Alternatively, when combined with MM18, Tetraether provided some resistance; this effect decreased when the colipid proportion increased, the highest resistance being reached at a lipid/colipid molar ratio of 10/1 (Figure 4B2). Of note, in every instance, dextran sulfate addition did not allow 100% restoration of fluorescence, indicating that this counteranion was unable to achieve full DNA release, even when used at high dose. Taken together, these results showed that Tetraether can exert different, even opposite, effects depending on the cationic lipid combined. Notably, it allows improving DNA condensation, neutralization, and resistance to dissociation performances

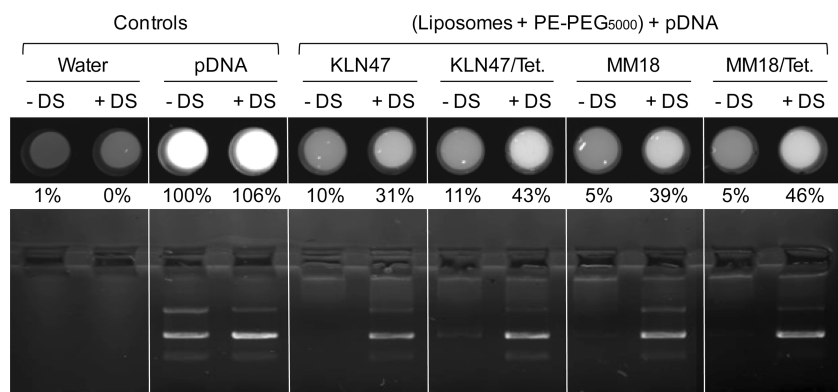


Figure 5. DNA entrapment within highly concentrated, sterically stabilized, lipid/DNA complexes. KLN47 and MM18-based formulations, incorporating or not Tetraether (in a lipid/colipid molar ratio of 10/1), were first supplemented with PE-PEG₅₀₀₀ (in a lipid-PEG/DNA mass ratio of 2/1); they were next mixed in water with pGL3-Ctrl in order to form complexes at CR3. After 10 min at RT, each complex was mixed either with dextran sulfate (“+DS”, 25 $\mu\text{g}/\mu\text{g}$ DNA) or with water (“-DS”). The top panel shows fluorescence photography of wells under UV transillumination with corresponding relative fluorescence intensities indicated underneath (100% being set for naked, uncomplexed, pDNA); the bottom panel shows agarose gel electrophoresis shift assays. The arrows indicate three different pDNA topological conformations (relaxed, coiled, and supercoiled forms, from top to bottom, respectively).

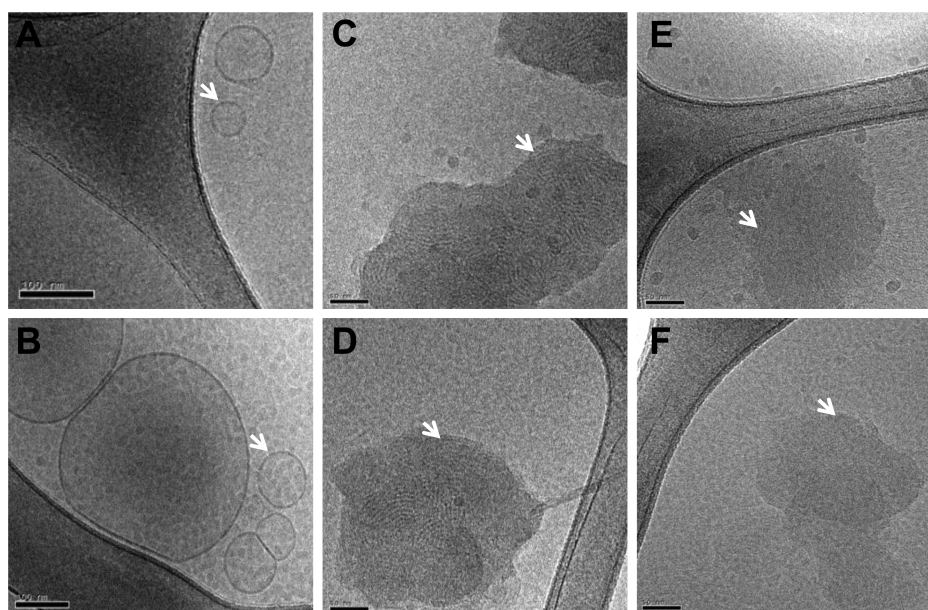


Figure 6. Cryo-TEM micrographs of MM18/Tetraether 10/1 (top panels) and KLN47/Tetraether 10/1 (bottom panels). Lipid concentration was 1 mg/mL. Archaeosomes (left panels; scale bar, 100 nm) and corresponding archaeoplexes (middle and right panels; scale bar, 50 nm). Arrows indicate unilamellar structures in A and B, multilamellar complexes in C and D, and nonlamellar domains in E and F.

of MM18, the lowest lipid/colipid molar ratio being the most favorable from those points of view.

DNA condensation and neutralization were also evaluated under experimental conditions compatible with local gene delivery *in vivo* (notably nasal instillation). Here, each lipid-based formulation was first supplemented with PE-PEG₅₀₀₀ before mixing with DNA. Condensation assays were performed thereafter (Figure 5).

The results showed that DNA was efficiently entrapped within all the complexes studied, even within MM18-based lipoplexes. Indeed, only a low fluorescence was observed in each well and residual signals varied in the range of 5 to 10% relative fluorescence unit (RFU). Here, the absence of NaCl (as compared with our previous assay (Figure 4)) favored electrostatic interactions between cationic lipids and DNA. Furthermore, PE-PEG₅₀₀₀ did not abolish the DNA con-

densation ability of any lipid formulation. The addition of dextran sulfate allowed restoring some free (uncomplexed) DNA. However, although a high dose of this counteranion was used, DNA release was only partial, as fluorescence only increased from 31 to 46%. This could be partly ascribed to the stabilizer, as it may limit the interactions between dextran sulfate and the preformed complexes. On agarose gel, different DNA bands (corresponding to different pDNA conformations) were recovered and some fluorescence was also observed in each well. This indicated that DNA was intact (no apparent smear) and that all complexes exhibited high resistance to dissociation. Thus, sterically stabilized complexes could be obtained from any lipid-based formulation using the same PE-PEG₅₀₀₀ amount, thereby allowing a proper comparative evaluation of their respective *in vivo* transfection activity.

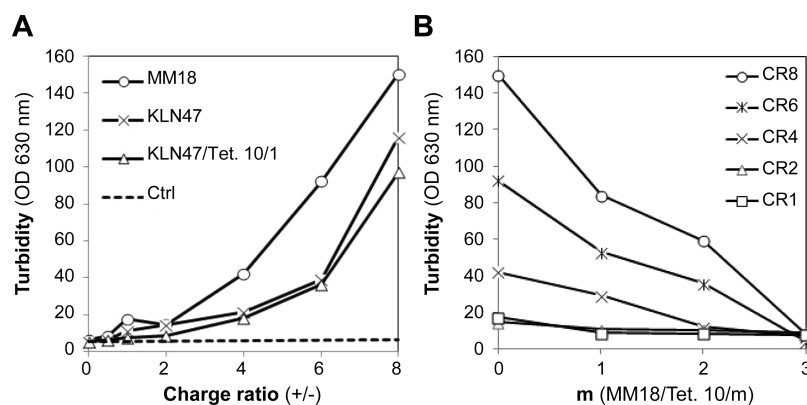


Figure 7. Aggregation of lipid/DNA complexes in the presence of serum (10% final) as a function of charge ratio (A) and lipid/colipid molar ratio (B). As controls (Ctrl), complexes were mixed with 0.9% NaCl instead of serum. *m*, proportion of Tetraether (means with *n* = 3).

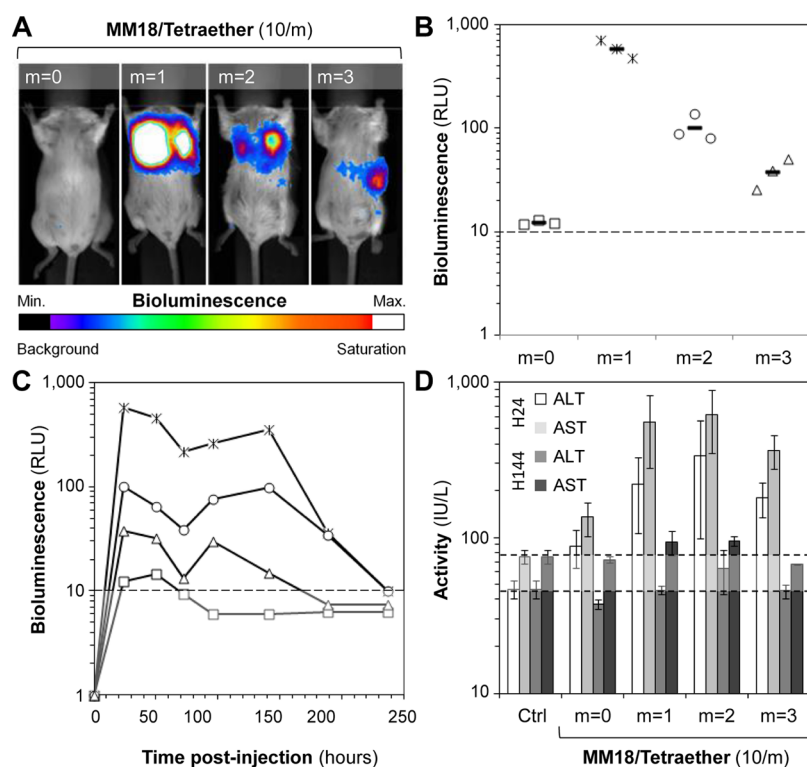


Figure 8. *In vivo* gene transfer activity of MM18 as compared with MM18/Tetraether (in a molar ratio of 10/1, 10/2, or 10/3) following iv injection in mice. Representative *in vivo* bioluminescence images (A); intensity of bioluminescence signals measured 24 h postinjection (H24) in the lung area (B); kinetic of *in vivo* bioluminescence (C); and quantification of ALT and AST plasma activities at early (H24) and late (H144) stages postinjection (D). In panels B and C, bioluminescence signals are expressed as relative light units (RLU) and the symbol code is the same. In panel D, transaminase activities are expressed as International Units per liter (IU/L). Mice injected with naked pDNA were used as controls (Ctrl). The dashed lines indicate the threshold values in each case. *m*, proportion of Tetraether (means with *n* = 3).

Overall, all liposomes and archaeosomes demonstrated variable but at least minimal ability to bind (neutralization) as well as condense (compaction) DNA, under experimental conditions compatible with *in vivo* administration procedures.

3.2.5. Cryo-TEM Imaging of Archaeosomes and Archaeoplexes. Cryo-TEM was employed to investigate the morphology of the formulations incorporating Tetraether in the absence (archaeosomes) or presence (archaeoplexes formed at CR3) of salmon sperm DNA (Figure 6).

Few unilamellar structures were observed with both formulations including Tetraether as a colipid (Figure 6, panels A and B). KLN47 or MM18-based archaeoplexes were characterized by both multilamellar (panels C and D) and

nonlamellar (panels E and F) supramolecular structures. The multilamellar arrangements (panels C and D) likely corresponded to multilayer stackings of amphiphiles intercalated with DNA strands, as previously reported in the literature.³⁵

3.2.6. Aggregation of Lipid/DNA Complexes in the Presence of Serum. An aggregation assay was worked out that consisted of incubating complexes (prepared under conditions compatible for iv injection) with fetal bovine serum (FBS), as detailed in the Experimental Section. This should mimic the conditions that complexes encounter upon injection in the bloodstream. Briefly, complexes were formed at several charge ratios ranging from 0.5 to 8.0 by mixing, in 0.9% NaCl, a constant amount of pDNA with increasing quantities of

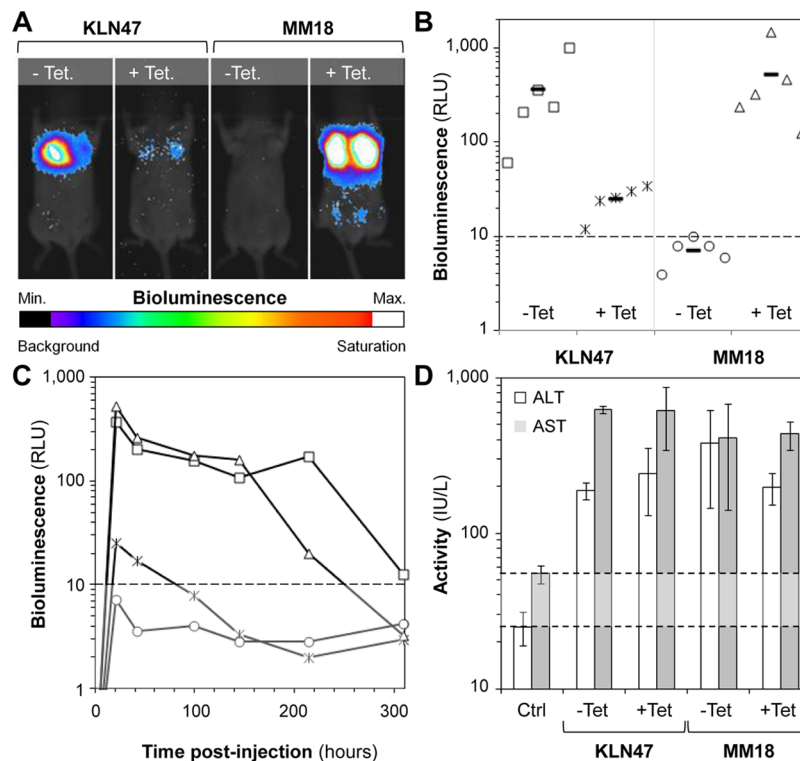


Figure 9. *In vivo* gene transfer activity of MM18 and KLN47 as compared with MM18/Tetraether 10/1 and KLN47/Tetraether 10/1 following *iv* injection in mice. Representative *in vivo* bioluminescence images (A); intensity of bioluminescence signals collected 24 h postinjection (H24) in the lung area (B); kinetics of *in vivo* bioluminescence (C); and quantification of ALT and AST plasma activities at an early (H24) stage (D). In panels B and C, bioluminescence signals are expressed as relative light units (RLU) and the symbol code is the same. In panel D, transaminase activities are expressed as International Units per liter (IU/L). Mice injected with naked pDNA were used as controls (Ctrl). The dashed lines indicate the threshold values in each case (means with $n = 5$).

a given lipid formulation. After addition of serum and incubation at 37 °C for 30 min, optical densities were measured at 630 nm (Figure 7; Figure S4 in the Supporting Information shows the results obtained when using water rather than 0.9% NaCl).

As shown in Figure 7, all the formulations aggregated in the presence of serum, although with various intensities. This aggregation was all the more important as the charge ratio was high. Considering MM18-based formulations, we observed that the higher the colipid proportion, the less intense the aggregation. Hence, Tetraether can modulate aggregation between complexes and/or with serum proteins, a parameter related to fusogenicity which may play a critical role in biodistribution and transfection activity following *iv* injection.

3.3. *In Vivo* Gene Transfer Studies. Next, lipoplexes and archaeoplexes were used to perform *in vivo* gene transfer experiments in mice. Considering *iv* delivery, three Tetraether proportions in mixture with one given cationic lipid were first evaluated. Next, the transfection activities of two different cationic lipids combined with Tetraether were compared, following *iv* injection and *i.n.* deposition. In all these tests, a luciferase-encoding CpG-free pDNA (pGM144) was used, as it was previously shown to allow efficient and sustained transgene expression *in vivo*.³²

3.3.1. Intravenous Administration. **3.3.1.1. Comparative Evaluation of the Transfection Activity of MM18 Used Alone or Combined with Tetraether at Different Proportions.** The MM18 cationic lipid formulated or not with Tetraether (in a lipid/colipid molar ratio of 10/1, 10/2, or 10/3) was mixed, in 0.9% NaCl, with the pGM144 pDNA in order to form

complexes at CR4. The lipoplexes and archaeoplexes thus obtained were then *iv* injected in a series of mice. Various evaluations were subsequently performed for several days (Figure 8).

Following *iv* injection, animals were subjected to a series of bioluminescence imaging for several days. This revealed that, from 24 h postinjection, the tested formulations could mediate some luciferase expression with very different levels of efficiency. Depending on the administered formulation, different areas of the animal body displayed some bioluminescence, suggesting that different tissues/organs had taken up some pDNA and expressed the luciferase reporter gene (Figure S5 in the Supporting Information). While the signals observed in the chest area originated most probably from the lungs (as we have previously observed with other lipid-based systems^{7,8,30}) and those in the left flank from the spleen, the signals observed from other parts of the body were more difficult to attribute to precise organs or tissues. Moreover, such “accessory” bioluminescent spots were not systematically observed in all the animals within a single lot. Overall, the most sustainable bioluminescence signals were those likely originating from the lungs; 5 days after treatment, they were the only ones persisting.

When focusing on bioluminescence signals collected from the thoracic area, the different formulations mediated quite different levels of reporter gene expression. MM18-based lipoplexes were unable to efficiently transfect the lungs (or another organ). Indeed, no bioluminescence signals were detected at the level of the whole body. On the contrary, the combination of MM18 with Tetraether allowed obtaining

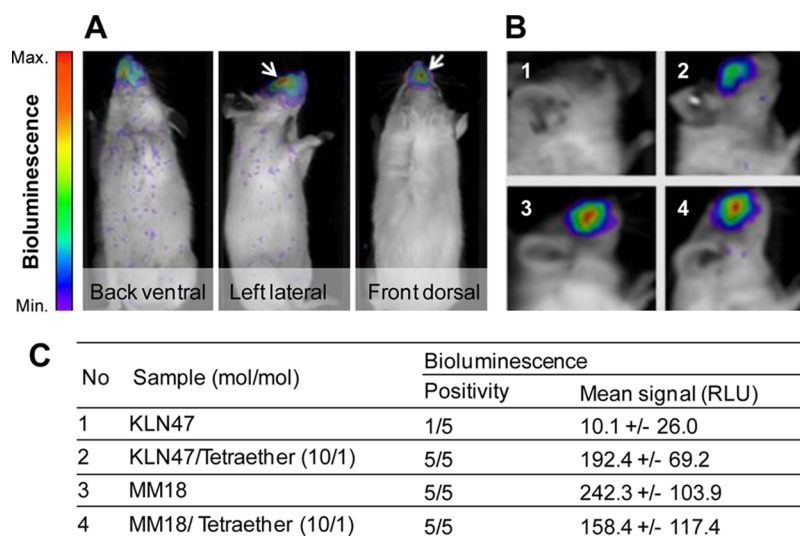


Figure 10. *In vivo* gene transfer activity of MM18 and KLN47 as compared with MM18/Tetraether 10/1 and KLN47/Tetraether 10/1 following i.n. deposition in mice. Representative *in vivo* bioluminescence images from the whole body of a whole mouse according to three body positions (A); bioluminescence imaging, 24 h postadministration, of the head of animals (B); and table summarizing the results (positivity, proportion of the animals showing a detectable bioluminescence signal) (C). The arrows point toward the right nostril (where instillation was performed).

bioluminescence signals that reached high levels of intensity. Overall, 24 h after injection, the formulations could be ranked from the most efficient to the least as follows: MM18/Tetraether 10/1 > MM18/Tetraether 10/2 > MM18/Tetraether 10/3 > MM18. This ranking remained the same until at least 250 h postinjection. When considering the whole body bioluminescence, it appeared that the colipid amount mixed with MM18 strongly influenced the *in vivo* transfection profile. Indeed, at a molar ratio of 10/1, intense bioluminescence signals were mostly observed in the thoracic area. At a molar ratio of 10/2, such bioluminescence signals were also obtained but they were much weaker and a signal from the spleen was also detectable. At a molar ratio of 10/3, no bioluminescence signals could be detected from the lungs anymore whereas those from the spleen were dominating. Regarding toxicity, some animals exhibited some signs of stress, especially those injected with archaeoplexes. A single death occurred, immediately after blood collection performed 24 h after injection. Measurements of ALT/AST transaminase activities in plasma indicated that the formulations effective for *in vivo* transfection also led to some transient liver injuries. Indeed, MM18-based lipoplexes, which were ineffective, induced no (or only little) detectable toxicity. On the other hand, when MM18 was formulated with Tetraether, transfection was efficient but it also induced some hepatotoxicity. Interestingly, whereas the peak of *in vivo* bioluminescence was obtained at a molar ratio of 10/1, the highest toxicity was reached at a molar ratio of 10/2. It should be stressed that the observed hepatic injuries were transient. Indeed, 6 days after injection, ALT/AST dosages exhibited normal values, regardless of the administered formulation.

3.3.1.2. Comparative Evaluation of the Transfection Activity of KLN47 and MM18 Combined or Not with Tetraether. The aforementioned results showed that, via iv route, Tetraether colipid was the most beneficial for transfecting mouse lungs when it was combined in a small proportion with the MM18 cationic lipid. Next, we wondered whether such a benefit could be also obtained when using another type of cationic lipid that, contrary to MM18, can be

effective on its own. For this purpose, we chose the arsonium-containing lipophosphoramidate KLN47.^{7,30} Thus, KLN47 and MM18, combined or not with Tetraether (in a molar ratio of 10/1), were used to complex, in 0.9% NaCl, the pGM144 pDNA at CR4. The obtained complexes were iv injected in other mice in order to compare their respective *in vivo* transfection activity (Figure 9).

The various complexes demonstrated very different abilities to mediate luciferase gene expression in mice *in vivo*. Bioluminescence signals mainly stemmed from the thorax, indicating that the transfection most likely took place in the lungs rather than in another body area. MM18-based lipoplexes remained ineffective (as observed before, see Figure 8) whereas KLN47-based lipoplexes demonstrated high gene transfection efficiency (as previously reported³⁰). As regards archaeoplexes, those incorporating KLN47 demonstrated only a very weak efficiency while those incorporating MM18 mediated bioluminescence signals as intense as those obtained when using KLN47-based lipoplexes. Overall, 24 h after injection, the ranking order of formulations in decreasing order of efficiency was as follows: MM18/Tetraether 10/1 > KLN47 ≫ KLN47/Tetraether 10/1 ~ MM18. This ranking remained identical until at least 150 h postinjection. Of note, luciferase expression was observed for ~300 h, a slightly longer duration than that observed in our previous experiment. This difference might arise from the fact that the pDNA batches were not the same for those two experiments. As regards toxicity, measurements of ALT/AST plasma activities indicated that all formulations induced some level of hepatotoxicity; however, these injuries were transient, a fact in agreement with previous investigations (this study and ref 8).

3.3.2. Intranasal Administration. Finally, MM18 and KLN47, combined or not with Tetraether (in a molar ratio of 10/1), were used for transfection of the nasal epithelium via intranasal instillation, the nose providing an easy access to the airway epithelium. As such a local administration requires the use of highly concentrated lipid/DNA mixtures, liposomes/archaeosomes were first combined, for colloidal stabilization purpose, with PE-PEG₅₀₀₀ before being mixed in water with

pGM144 pDNA at CR3. The obtained complexes were then delivered into the nostril of a last series of mice. The results are shown in Figure 10.

This administration procedure showed that local gene delivery to the nasal epithelium can be achieved with some of the evaluated complexes: a bioluminescence signal was detected around the deposition site whereas no signal was detectable from any other part of the whole animal. KLN47-based lipoplexes were the least effective by this way, as no or only weak bioluminescence signals were detected. On the contrary, when combined with Tetraether, this cationic lipid allowed measuring clearly positive luciferase expression levels. As concerns MM18-based lipoplexes and MM18-based archaeoplexes, they were both clearly efficient for gene transfection. Of note, all effective complexes led to reporter gene expression levels of the same order of magnitude. Finally, no morbidity nor mortality was observed when using such a delivery route, in accordance with previous studies.³⁶

4. DISCUSSION

Among the numerous parameters determining the efficiency of nonviral gene transfection *in vivo*, the chemical structure of the delivery system, its formulation preparation, and the administration route are crucial.³⁷ A formulation suitable for iv injection may be inappropriate for local administrations (such as i.n., intratracheal, or intratissue delivery) and *vice versa*. Indeed, environmental constraints specific to each route (e.g., different biological media) may impact in different ways the bioavailability and functionality of any drug.³⁸ Thus, the physicochemical parameters of synthetic gene delivery systems should be fine-tuned according to the type of application. To date, most of the efforts to optimize lipid-based formulations with regard to delivery pathways have focused on cationic lipids themselves whereas fewer studies have investigated the use of original colipids with the aim of improving *in vivo* lipofection. In previous works, we have studied original cationic liposomes, termed archaeosomes, based on combinations of neutral/cationic bilayer-forming lipids with archaeobacterial synthetic tetraether-type bipolar lipids. Tetraether proved to be a new alternative for modulating the lipid membrane fluidity of the complexes they formed with DNA and archaeoplexes demonstrated promising *in vitro* gene transfection abilities.^{27,28,31} In the present study, we evaluated the effects of Tetraether (used as a colipid) on the *in vivo* gene transfer activity of two monocationic amphiphiles. A series of analytical assays were performed and *in vivo* gene transfection experiments were conducted in mice using two different delivery routes.

The different compounds synthesized in this study were obtained in good yield and purity (>98%), notably MM18 whose synthesis is reported here for the first time (Scheme 1). They were next prepared as liposomes. It is noteworthy that Tetraether, when used alone, was never demonstrated able to self-organize as micelles or liposomes (data not shown); a cationic lipid incorporating two aliphatic chains was always required to obtain Tetraether-based lipid assemblies. This may be related to the unconventional chemical structure of this compound as it is a monolayer-forming lipid (Figure 1). Here, archaeosomes were obtained by mixing Tetraether with either KLN47 or MM18. One main hurdle for *in vivo* nonviral gene delivery is related to the maximal volume that can be administered, at once, in a small animal like a mouse. Conversely, quite high quantities of materials (vector and

DNA) need to be delivered in order to obtain sufficient transgene expression. Hence, highly concentrated liposomal and lipid/DNA mixtures are required. The feasibility to prepare concentrated and stable formulations was first investigated. We found that aqueous solutions of the various lipid-based formulations considered can be obtained up to concentrations as high as 20 nmol[+]/ μ L of cationic lipid. The incorporation of Tetraether strongly impacted the size but did not impact (or only slightly impacted) the surface charge (Table 1). Importantly, all those preparations demonstrated long-term stability, at least for one month (when stored at 4 °C), without any obvious variations of their size and surface charge characteristics and while retaining their transfection ability *in vitro* (Figure S1 in the Supporting Information) and *in vivo* (see below). Overall, these findings validated the protocol used for preparing highly concentrated liposomal solutions from the various lipids studied herein. This is an important point to emphasize as transfection reagents do not always meet this requirement; indeed, instability of formulations is a major drawback for the successful and widespread use of any given lipid-based system.

Next, the *in vivo* transfection activity of the various formulations studied herein was evaluated in mice under different experimental conditions. Given our interest in nonviral gene therapy for the treatment of diseases like cystic fibrosis, we focused our investigations on gene transfer to the lungs (via iv injection into the tail vein) on the one hand and to the nasal epithelium (via local deposition into the nostril) on the other. Besides varying the *in vivo* administration route, we also determined the impacts of modulating the lipid/colipid molar proportion (of 10/1, 10/2, or 10/3) and the type of cationic lipid used (KLN47 or MM18). Preliminary *in vitro* evaluations confirmed that all these lipid-based formulations exhibited good gene transfer efficiencies into a series of eukaryotic cells, notably two human lung epithelial cell lines (A549 and 16HBE; data not shown). It is also noteworthy that we report here for the first time the evaluation of the *in vivo* gene transfection activity of MM18, a glycine betaine cationic lipid.

Following iv delivery, MM18-based lipoplexes did not mediate any detectable reporter gene expression (Figure 8). This might be ascribed to some properties unsuited for systemic delivery, in particular a relatively limited ability to condense (Figure 3) and neutralize (Figure 4) pDNA. In contrast, MM18-based archaeosomes were much more efficient from those two points of view, especially at the charge ratios used for conducting *in vivo* experiments. Accordingly, MM18-based archaeoplexes demonstrated some transfection efficiency in mice *in vivo*, bioluminescence signals being detected in different areas of the animal body. However, depending on the Tetraether proportion mixed with MM18, the *in vivo* transfection patterns showed substantial differences. Among the three lipid/colipid molar ratios we have evaluated, the 10/1 (rather than the 10/2 and the 10/3) was identified as the most efficient for *in vivo* gene transfection, especially into the lungs (Figure 8A). This is actually in agreement with previous *in vitro* transfection experiments that showed that Tetraether was more advantageous when combined in a relatively low proportion with a cationic lipid.²⁸ Besides the thorax, other body parts displayed some bioluminescence (although at lower intensities), especially when increasing the colipid proportion. Indeed, it appears that MM18/Tetraether molar ratio determined a balance between gene transfer into the lungs and transfection into other organs or tissues. This finding may

be explained in different ways. Besides pGM144 pDNA characteristics which obviously play a role in transfection efficiency (especially plasmid size and promoter/enhancer elements governing the luciferase gene expression), a series of parameters related to the vector itself can be pointed out. It is generally recognized that the size of nanoparticles developed for iv delivery should vary in a precise range. Systemic delivery (by tail vein injection) of lipid/DNA complexes has previously been reported to permit gene transfection into the lungs, possibly thanks to their accumulation in the pulmonary microvasculature (as it is the first one encountered via this route).^{7,39–41} The underlying transfection mechanism may involve interactions between the lipid/DNA complexes and serum components, leading to aggregation and size increase with subsequent accumulation and retention into the lung microcirculation.⁴¹ As regards lipid/DNA complexes escaping from the pulmonary microvasculature, their size might then determine their distribution between the liver and the spleen, the smaller ones ($< \sim 70$ nm⁴²) accumulating preferentially in the liver and the larger ones ($> \sim 200$ nm⁴³) undergoing mechanical filtration into the spleen. Accordingly, no bioluminescence was observed from the liver whereas a signal could be detected from the spleen, especially when using archaeoplexes incorporating the highest Tetraether proportion (10/3) (Figure 8 and Figure S5 in the Supporting Information). Interestingly, such archaeoplexes had also the lowest propensity to aggregate in the presence of serum (Figure 7), possibly through a reduction of their fusogenic properties.^{44,45} Altogether, these findings suggest that Tetraether proportion may have strong modulating effects on pDNA interactions, size, and aggregation of resulting lipid/DNA complexes, a variety of physicochemical parameters which in turn may influence both the *in vivo* biodistribution and the transfection pattern at the whole body scale. It is hypothesized that, at a molar ratio of 10/1, Tetraether allowed an ideal compromise to be reached between stability of the lipid/DNA complexes (required in the bloodstream during trafficking toward the target organ/tissue) and dismantling ability (required inside the target cells, especially for endosomal escape and subsequent pDNA release into the cytoplasm), such a compromise leading to a highly efficient transfection of the lungs *in vivo*.

We next undertook to comparatively evaluate the *in vivo* transfection efficiency of KLN47 and MM18 liposomes as well as of the corresponding archaeosomes. Here, given our above-mentioned findings, the lipid/colipid molar ratio was set at 10/1 for both archaeosomes. Their complexes with the luciferase-encoding pGM144 were administered via tail vein injection into the bloodstream of another series of mice, and bioluminescence imaging was repeatedly performed during several days (Figure 9). In accordance with previous results (Figure 8), MM18-based lipoplexes were inefficient whereas corresponding archaeoplexes demonstrated high transfection efficiencies. KLN47-based lipoplexes also mediated lung reporter gene expression, as previously reported,^{7,30} with bioluminescence signals as strong as those measured when using MM18-based archaeoplexes. Surprisingly, when using KLN47-based archaeoplexes, a dramatic decrease in transfection efficiency was observed as compared with corresponding complexes devoid of Tetraether. Thus, depending on the type of cationic lipid with which it was combined, Tetraether demonstrated either a beneficial or on the contrary a strongly deleterious effect on *in vivo* gene transfection efficiency. Such a dual effect likely results

from some structural characteristics and/or physicochemical properties peculiar to each cationic lipid. KLN47 and MM18 are two monocationic lipids incorporating oleic chains, but their headgroups and linkers are different (Figure 1). It is noteworthy that aqueous dispersions of archaeosomes were more difficult to obtain with KLN47 than with MM18, probably because of differences in hydration and/or lipid mixing properties. Interestingly, no obvious differences were observed between lipoplexes and archaeoplexes as regards the lipid/DNA structures formed (Figure 6). Thus, the differences observed in gene transfer efficiency *in vivo* (via the iv route) when using the two types of lipoplexes and their corresponding archaeoplexes were probably not associated with differences in terms of DNA-vesicle association. On the contrary, when considering the lyotropic phases formed by liposomes and archaeosomes, an obvious difference was noticed as, in the case of MM18, the phase changed from hexagonal (liposomes) to lamellar (archaeosomes) whereas, in the case of KLN47, a lamellar phase was observed both with liposomes and archaeosomes (Figure 2). To explain the observed difference in gene transfection efficiencies, it is hypothesized that Tetraether might favor a reorganization of the membranes during cell transfection, especially inside the endosomal compartment. As concerns MM18/Tetraether, this should allow the formation of inverted hexagonal phases (Figure 2), a more fusogenic supramolecular organization facilitating the endosomal escape of pDNA.⁸

Next, we used the intranasal (i.n.) route to determine, in the context of local administration to the airway epithelium, the *in vivo* transfection efficiency of KLN47 and MM18 mixed or not with Tetraether (at a lipid/colipid molar ratio of 10/1). Although i.n. administration obviously does not allow full assessment of the potential of any given gene transfer agent for correction of the cystic fibrosis pulmonary complications,³⁶ it can nevertheless be used as a first step before performing more complicated experiments involving local delivery to the lower airways. Indeed, nasal instillation is an attractive method as (i) it is quite easy to perform and is noninvasive and non-surgery-based; (ii) the target tissue belongs to the respiratory epithelium; (iii) lower bioluminescence signals can be collected as the transfection site (the nasal epithelium) is less deep inside the body than the (intrathoracic) lungs. However, this delivery route also shows some technical limitations. The maximal volume that can be delivered at once via the i.n. route is much smaller than via the iv route. As minimal quantities of materials (lipid and DNA) need to be delivered, lipid/DNA mixtures must be prepared at high concentration. Colloidal stability constitutes a crucial parameter as any aggregation/precipitation of the lipid/DNA complexes would lead to a dramatic loss of their transfection efficiency.⁴⁶ Indeed, no bioluminescence signal was observed when nonstabilized complexes were delivered into the nostrils of animals, regardless of the lipid-based formulation used (data not shown). For all these reasons, we used here a PEGylated lipid derivative to sterically stabilize highly concentrated lipid/DNA complexes, which were characterized by a CR3 and a DNA concentration as high as 1 $\mu\text{g}/\mu\text{L}$ (Table 3 and Figure 5). The results (Figure 10) were quite different from those obtained following the iv route, highlighting that no obvious correlation can be delineated between the transfection abilities of a given lipid formulation via the iv route on the one hand and the i.n. route on the other. This shows the importance of not only the chemical composition of the formulations but also the procedure used

for their preparation and administration. Indeed, whereas MM18-based lipoplexes did not show any efficiency when delivered via *iv* route, they were efficient via *i.n.* (as well as when combined with Tetraether). The ionic strength was an obvious difference between the formulations prepared for those two routes, which can strongly impact DNA condensation ability, as evidenced for MM18 (Figures 4 and 5). KLN47-based lipoplexes were efficient via *iv* but they were not via *i.n.* On the contrary, KLN47-based archaeoplexes showed only very weak efficiency via *iv* whereas they reached some efficiency via *i.n.* Thus, Tetraether colipid might confer KLN47 with some properties useful for gene transfection in the context of *i.n.* deposition but detrimental in the context of *iv* injection. Taken together, these results illustrate the importance of a fine-tuned optimization taking into account multiple parameters of the lipid-based system depending on the type of application.

Finally, as concerns safety, it is first noteworthy that the mice exhibited no major clinical adverse effects. However, following *iv* injection, all formulations elicited an acute (but transient) release in blood of the ALT/AST liver enzymes. An increase of these enzyme activities (which did not exceed 10-fold the normal values) was noticed at an early time point (~24 h postinjection; Figures 8D and 9D), but it was transient as normal values were recovered at late time points (~6 days postinjection; Figure 8D). Thus, hepatic cytolysis was not dramatic, and, in every instance, it was fully reversible in a few days. Interestingly, MM18/Tetraether 10/1 induced an acute toxicity (at day 1) which was no longer observed at day 6 while high reporter gene expression was still measured (Figure 8). Altogether, all complexes were relatively well-tolerated by the animals. It may be expected that the use of a pH-cleavable tetraether derivative, which could be also more easily degraded inside the cells, may allow reducing the side effects in the host *in vivo*.

5. CONCLUSION

This work emphasizes that successful *in vivo* gene transfection following a given route of administration requires the specific optimization of various parameters related to the vector formulations including the type of cationic lipid as well as the proportion of colipid. Modulation of these parameters may result in highly efficient transfection of specific tissues/organs, especially the lungs. Nowadays, most nonviral gene delivery systems incorporate several components to achieve multiple tasks, in order to overcome the various successive barriers encountered during *in vivo* transfection. Given its particular chemical structure and physicochemical properties, Tetraether colipid could provide lipid/DNA complexes with additional properties (notably rigidity/stability) advantageous for lung-directed gene therapy, especially via nebulization in the context of cystic fibrosis. Current studies are being performed to test this assumption. In a broader perspective, our original Tetraether derivative may offer novel possibilities for fine-tuning lipid-based systems to be used for other applications.

■ ASSOCIATED CONTENT

● Supporting Information

In vitro transfection efficiency and cell viability using lipid-based formulations cold-stored (at 4 °C) for several months; time course of DNA condensation within lipoplexes and archaeoplexes as prepared for *iv* injection; DNA retardations by agarose gel electrophoresis using lipoplexes and archaeoplexes as prepared for *iv* injection; aggregation of lipoplexes and

archaeoplexes in the presence of serum (test in water); various bioluminescence spots from mice injected with MM18-based archaeoplexes. This material is available free of charge via the Internet at <http://pubs.acs.org>.

■ AUTHOR INFORMATION

Corresponding Authors

*(T.L.G.) Phone: +33 (0)298018103. Fax: +33 (0)298467910. E-mail: tony.legall@univ-brest.fr.

*(T.B.) Phone: +33 (0)223238060. Fax: +33 (0)223238046. E-mail: thierry.benvegnu@ensc-rennes.fr.

*(T.M.) Phone: +33 (0)298018080. Fax: +33 (0)298467910. E-mail: tristan.montier@univ-brest.fr.

Notes

The authors declare no competing financial interest.

■ ACKNOWLEDGMENTS

The authors thank Dr. Olivier Lambert for performing cryo-TEM analyses (UMR CNRS 5248 “Chimie et Biologie des Membranes et des Nano-objets”, Université de Bordeaux, France). This work was supported by grants from “Association Française contre les Myopathies” (Evry, France), “Vaincre La Mucoviscidose” (Paris, France), “Association de Transfusion Sanguine et de Biogénétique Gaétan Saleün” (Brest, France), “Conseil Régional de Bretagne”, and “Brest Métropole Océane”.

■ ABBREVIATIONS USED

CR, charge ratio; *i.n.*, intranasal; *ip*, intraperitoneal; *iv*, intravenous; DOPE, dioleoyl phosphatidylethanolamine; pDNA, plasmid DNA; PEG, polyethylene glycol; RT, room temperature; Tet, Tetraether

■ REFERENCES

- (1) Wells, D. J. Gene therapy progress and prospects: electroporation and other physical methods. *Gene Ther.* **2004**, *11*, 1363–1369.
- (2) Guo, X.; Huang, L. Recent advances in nonviral vectors for gene delivery. *Acc. Chem. Res.* **2012**, *45*, 971–979.
- (3) Le Gall, T.; Baussanne, I.; Halder, S.; Carmoy, N.; Montier, T.; Lehn, P.; Decout, J. L. Synthesis and transfection properties of a series of lipidic neamine derivatives. *Bioconjugate Chem.* **2009**, *20*, 2032–2046.
- (4) Billiet, L.; Gomez, J.-P.; Berchel, M.; Jaffrès, P.-A.; Le Gall, T.; Montier, T.; Bertrand, E.; Cheradame, H.; Guégan, P.; Mével, M.; Pitard, B.; Benvegnu, T.; Lehn, P.; Pichon, C.; Midoux, P. Gene transfer by chemical vectors, and endocytosis routes of polyplexes, lipoplexes and lipopolyplexes in a myoblast cell line. *Biomaterials* **2012**, *33*, 2980–2990.
- (5) Berchel, M.; Le Gall, T.; Couthon-Gourvès, H.; Haelters, J.-P.; Montier, T.; Midoux, P.; Lehn, P.; Jaffrès, P.-A. Lipophosphonate/lipophosphoramidates: a family of synthetic vectors efficient for gene delivery. *Biochimie* **2012**, *94*, 33–41.
- (6) Loizeau, D.; Le Gall, T.; Mahfoudhi, S.; Berchel, M.; Maroto, A.; Yaouanc, J.-J.; Jaffrès, P.-A.; Lehn, P.; Deschamps, L.; Montier, T.; Giamarchi, P. Physicochemical properties of cationic lipophosphoramidates with an arsonium head group and various lipid chains: A structure-activity approach. *Biophys. Chem.* **2013**, *171*, 46–53.
- (7) Le Gall, T.; Loizeau, D.; Picquet, E.; Carmoy, N.; Yaouanc, J. J.; Burel-Deschamps, L.; Delepine, P.; Giamarchi, P.; Jaffrès, P. A.; Lehn, P.; Montier, T. A novel cationic lipophosphoramidate with diunsaturated lipid chains: synthesis, physicochemical properties, and transfection activities. *J. Med. Chem.* **2010**, 1496–1508.
- (8) Lindberg, M. F.; Carmoy, N.; Le Gall, T.; Fraix, A.; Berchel, M.; Lorilleux, C.; Couthon-Gourvès, H.; Bellaud, P.; Fautrel, A.; Jaffrès, P.-A.; Lehn, P.; Montier, T. The gene transfection properties of a

lipophosphoramidate derivative with two phytanyl chains. *Biomaterials* **2012**, *33*, 6240–6253.

(9) McLachlan, G.; Davidson, H.; Holder, E.; Davies, L. A.; Pringle, I. A.; Sumner-Jones, S. G.; Baker, A.; Tennant, P.; Gordon, C.; Vrettou, C.; Blundell, R.; Hyndman, L.; Stevenson, B.; Wilson, A.; Doherty, A.; Shaw, D. J.; Coles, R. L.; Painter, H.; Cheng, S. H.; Scheule, R. K.; Davies, J. C.; Innes, J. A.; Hyde, S. C.; Griesenbach, U.; Alton, E. W. F. W.; Boyd, A. C.; Porteous, D. J.; Gill, D. R.; Collie, D. D. S. Pre-clinical evaluation of three non-viral gene transfer agents for cystic fibrosis after aerosol delivery to the ovine lung. *Gene Ther.* **2011**, *18*, 996–1005.

(10) Griesenbach, U.; Alton, E. W. F. W. Current status and future directions of gene and cell therapy for cystic fibrosis. *BioDrugs* **2011**, *25*, 77–88.

(11) Griesenbach, U.; Alton, E. W. F. W. Progress in gene and cell therapy for cystic fibrosis lung disease. *Curr. Pharm. Des.* **2012**, *18*, 642–662.

(12) Xu, L.; Anchordoquy, T. Drug delivery trends in clinical trials and translational medicine: challenges and opportunities in the delivery of nucleic acid-based therapeutics. *J. Pharm. Sci.* **2011**, *100*, 38–52.

(13) Zhang, X.-X.; McIntosh, T. J.; Grinstaff, M. W. Functional lipids and lipoplexes for improved gene delivery. *Biochimie* **2012**, *94*, 42–58.

(14) McCarthy, H. O.; Wang, Y.; Mangipudi, S. S.; Hatefi, A. Advances with the use of bio-inspired vectors towards creation of artificial viruses. *Expert Opin. Drug Delivery* **2010**, *7*, 497–512.

(15) Le Gall, T.; Berchel, M.; Le Hir, S.; Fraix, A.; Salaün, J. Y.; Férec, C.; Lehn, P.; Jaffres, P.-A.; Montier, T. Arsonium-containing lipophosphoramides, poly-functional nano-carriers for simultaneous antibacterial action and eukaryotic cell transfection. *Adv. Healthcare Mater.* **2013**, *2*, 1513–1524.

(16) Bennett, M. J.; Nantz, M. H.; Balasubramaniam, R. P.; Gruenert, D. C.; Malone, R. W. Cholesterol enhances cationic liposome-mediated DNA transfection of human respiratory epithelial cells. *Biosci. Rep.* **1995**, *15*, 47–53.

(17) Litzinger, D. C.; Huang, L. Amphipathic poly(ethylene glycol) 5000-stabilized dioleoylphosphatidylethanolamine liposomes accumulate in spleen. *Biochim. Biophys. Acta* **1992**, *1127*, 249–254.

(18) Xu, Y.; Szoka, F. C., Jr. Mechanism of DNA release from cationic liposome/DNA complexes used in cell transfection. *Biochemistry* **1996**, *35*, 5616–5623.

(19) Zuhorn, I. S.; Oberle, V.; Visser, W. H.; Engberts, J. B. F. N.; Bakowsky, U.; Polushkin, E.; Hoekstra, D. Phase behavior of cationic amphiphiles and their mixtures with helper lipid influences lipoplex shape, DNA translocation, and transfection efficiency. *Biophys. J.* **2002**, *83*, 2096–2108.

(20) Koltover, I.; Salditt, T.; Rädler, J. O.; Safinya, C. R. An inverted hexagonal phase of cationic liposome-DNA complexes related to DNA release and delivery. *Science* **1998**, *281*, 78–81.

(21) Gaucheron, J.; Boulanger, C.; Santaella, C.; Sbirrazzuoli, N.; Boussif, O.; Vierling, P. In vitro cationic lipid-mediated gene delivery with fluorinated glycerophosphoethanolamine helper lipids. *Bioconjugate Chem.* **2001**, *12*, 949–963.

(22) Prata, C. A. H.; Li, Y.; Luo, D.; McIntosh, T. J.; Barthelemy, P.; Grinstaff, M. W. A new helper phospholipid for gene delivery. *Chem. Commun. (Camb.)* **2008**, 1566–1568.

(23) Kurosaki, T.; Kitahara, T.; Teshima, M.; Nishida, K.; Nakamura, J.; Nakashima, M.; To, H.; Hukuchi, H.; Hamamoto, T.; Sasaki, H. Exploitation of De Novo helper-lipids for effective gene delivery. *J. Pharm. Pharm. Sci.* **2008**, *11*, 56–67.

(24) Zeisig, R.; Röss, A.; Fichtner, I.; Walther, W. Lipoplexes with alkylphospholipid as new helper lipid for efficient in vitro and in vivo gene transfer in tumor therapy. *Cancer Gene Ther.* **2003**, *10*, 302–311.

(25) Mével, M.; Neveu, C.; Goncalves, C.; Yaouanc, J. J.; Pichon, C.; Jaffres, P. A.; Midoux, P. Novel neutral imidazole-lipophosphoramides for transfection assays. *Chem. Commun.* **2008**, 3124–3126.

(26) Huang, Z.; Li, W.; Szoka, F. C., Jr. Asymmetric 1-alkyl-2-acyl phosphatidylcholine: a helper lipid for enhanced non-viral gene delivery. *Int. J. Pharm.* **2012**, *427*, 64–70.

(27) Brard, M.; Richter, W.; Benvegno, T.; Plusquellec, D. Synthesis and supramolecular assemblies of bipolar archaeal glycolipid analogues containing a cis-1,3-disubstituted cyclopentane ring. *J. Am. Chem. Soc.* **2004**, *126*, 10003–10012.

(28) Réthoré, G.; Montier, T.; Le Gall, T.; Delépine, P.; Cammas-Marion, S.; Lemiègre, L.; Lehn, P.; Benvegno, T. Archaeosomes based on synthetic tetraether-like lipids as novel versatile gene delivery systems. *Chem. Comm. (Cambridge, England)* **2007**, 2054–2056.

(29) Montier, T.; Benvegno, T.; Jaffres, P. A.; Yaouanc, J. J.; Lehn, P. Progress in cationic lipid-mediated gene transfection: a series of bio-inspired lipids as an example. *Curr. Gene Ther.* **2008**, *8*, 296–312.

(30) Picquet, E.; Le Ny, K.; Delépine, P.; Montier, T.; Yaouanc, J. J.; Cartier, D.; des Abbayes, H.; Férec, C.; Clément, J. C. Cationic lipophosphoramidates and lipophosphoguanidines are very efficient for in vivo DNA delivery. *Bioconjugate Chem.* **2005**, *16*, 1051–1053.

(31) Brard, M.; Lainé, C.; Réthoré, G.; Laurent, I.; Neveu, C.; Lemiègre, L.; Benvegno, T. Synthesis of archaeal bipolar lipid analogues: a way to versatile drug/gene delivery systems. *J. Org. Chem.* **2007**, *72*, 8267–8279.

(32) Hyde, S. C.; Pringle, I. A.; Abdullah, S.; Lawton, A. E.; Davies, L. A.; Varathalingam, A.; Nunez-Alonso, G.; Green, A. M.; Bazzani, R. P.; Sumner-Jones, S. G.; Chan, M.; Li, H.; Yew, N. S.; Cheng, S. H.; Boyd, A. C.; Davies, J. C.; Griesenbach, U.; Porteous, D. J.; Sheppard, D. N.; Munkonge, F. M.; Alton, E. W.; Gill, D. R. CpG-free plasmids confer reduced inflammation and sustained pulmonary gene expression. *Nat. Biotechnol.* **2008**, *26*, 549–551.

(33) Ruponen, M.; Yla-Herttuala, S.; Urtti, A. Interactions of polymeric and liposomal gene delivery systems with extracellular glycosaminoglycans: physicochemical and transfection studies. *Biochim. Biophys. Acta* **1999**, *1415*, 331–341.

(34) Floch, V.; Legros, N.; Loisel, S.; Guillaume, C.; Guilbot, J.; Benvegno, T.; Ferrieres, V.; Plusquellec, D.; Férec, C. New biocompatible cationic amphiphiles derivative from glycine betaine: a novel family of efficient nonviral gene transfer agents. *Biochem. Biophys. Res. Commun.* **1998**, *251*, 360–365.

(35) Battersby, B. J.; Grimm, R.; Huebner, S.; Cevc, G. Evidence for three-dimensional interlayer correlations in cationic lipid-DNA complexes as observed by cryo-electron microscopy. *Biochim. Biophys. Acta* **1998**, *1372*, 379–383.

(36) Griesenbach, U.; Sumner-Jones, S. G.; Holder, E.; Munkonge, F. M.; Wodehouse, T.; Smith, S. N.; Wasowicz, M. Y.; Pringle, I.; Casamayor, I.; Chan, M.; Coles, R.; Cornish, N.; Dewar, A.; Doherty, A.; Farley, R.; Green, A.-M.; Jones, B. L.; Larsen, M. D. B.; Lawton, A. E.; Manvell, M.; Painter, H.; Singh, C.; Somerton, L.; Stevenson, B.; Varathalingam, A.; Siegel, C.; Scheule, R. K.; Cheng, S. H.; Davies, J. C.; Porteous, D. J.; Gill, D. R.; Boyd, A. C.; Hyde, S. C.; Alton, E. W. F. W. Limitations of the murine nose in the development of nonviral airway gene transfer. *Am. J. Respir. Cell Mol. Biol.* **2010**, *43*, 46–54.

(37) Delépine, P.; Montier, T.; Guillaume, C.; Vaysse, L.; Le Pape, A.; Férec, C. Visualization of the transgene distribution according to the administration route allows prediction of the transfection efficacy and validation of the results obtained. *Gene Ther.* **2002**, *9*, 736–739.

(38) Montier, T.; Delépine, P.; Pichon, C.; Férec, C.; Porteous, D. J.; Midoux, P. Non-viral vectors in cystic fibrosis gene therapy: progress and challenges. *Trends Biotechnol.* **2004**, *22*, 586–592.

(39) Griesenbach, U.; Chonn, A.; Cassady, R.; Hannam, V.; Ackerley, C.; Post, M.; Tanswell, A. K.; Olek, K.; O'Brodovich, H.; Tsui, L.-C. Comparison between intratracheal and intravenous administration of liposome-DNA complexes for cystic fibrosis lung gene therapy. *Gene Ther.* **1998**, *5*, 181–188.

(40) Delépine, P.; Guillaume, C.; Montier, T.; Clément, J. C.; Yaouanc, J. J.; Des Abbayes, H.; Berthou, F.; Le Pape, A.; Férec, C. Biodistribution study of phosphonolipids: a class of non-viral vectors efficient in mice lung-directed gene transfer. *J. Gene Med.* **2003**, *5*, 600–608.

(41) Li, S.; Tseng, W. C.; Stolz, D. B.; Wu, S. P.; Watkins, S. C.; Huang, L. Dynamic changes in the characteristics of cationic lipidic vectors after exposure to mouse serum: implications for intravenous lipofection. *Gene Ther.* **1999**, *6*, 585–594.

(42) Litzinger, D. C.; Buiting, A. M.; van Rooijen, N.; Huang, L. Effect of liposome size on the circulation time and intraorgan distribution of amphipathic poly(ethylene glycol)-containing liposomes. *Biochim. Biophys. Acta* **1994**, *1190*, 99–107.

(43) Kissel, T.; Roser, M. Influence of chemical surface-modification on the phagocytic properties of albumin nanoparticles. *Proc. Int. Symp. Controlled Release Bioact. Mater.* **1991**, *18*, 275–276.

(44) Chong, P. L.-G.; Ayesa, U.; Daswani, V. P.; Hur, E. C. On physical properties of tetraether lipid membranes: effects of cyclopentane rings. *Archaea* **2012**, *2012*, 138439.

(45) Elferink, M. G.; van Breemen, J.; Konings, W. N.; Driessen, A. J.; Wilschut, J. Slow fusion of liposomes composed of membrane-spanning lipids. *Chem. Phys. Lipids* **1997**, *88*, 37–43.

(46) Pitard, B.; Oudrhiri, N.; Lambert, O.; Vivien, E.; Masson, C.; Wetzter, B.; Hauchecorne, M.; Scherman, D.; Rigaud, J. L.; Vigneron, J. P.; Lehn, J. M.; Lehn, P. Sterically stabilized BGTC-based lipoplexes: structural features and gene transfection into the mouse airways in vivo. *J. Gene Med.* **2001**, *3*, 478–487.